JACS
JOURNAL OF THE AMERICAN CHEMICAL SOCIETY

Article

Imaging and profiling of proteins under oxidative conditions in cells and tissues by hydrogen-peroxide-responsive labeling

Hao Zhu, Tomonori Tamura, Alma Fujisawa, Yuki Nishikawa, Rong Cheng, Mikiko Takato, and Itaru Hamachi

J. Am. Chem. Soc., **Just Accepted Manuscript** • DOI: 10.1021/jacs.0c02547 • Publication Date (Web): 21 Aug 2020

Just Accepted

is published by the American Chemical Society. 1155 Sixteenth Street N.W., Washington, DC 20036

Imaging and profiling of proteins under oxidative conditions in cells and tissues by hydrogen-peroxide-responsive labeling

Hao Zhu,[1] Tomonori Tamura,[1,2] Alma Fujisawa,[1] Yuki Nishikawa,[1] Rong Cheng,[1] Mikiko Takato,[1] and Itaru Hamachi*[1,2]

[1]Department of Synthetic Chemistry and Biological Chemistry, Graduate School of Engineering, Kyoto University, Katsura, Nishikyo-ku, Kyoto 615-8510, Japan

[2]ERATO, Japan Science and Technology Agency (JST), 5 Sanbancho, Chiyoda-ku, Tokyo 102-0075, Japan

Correspondence should be addressed to I.H. (ihamachi@sbchem.kyoto-u.ac.jp)

Abstract

Reactive oxygen species (ROS) such as hydrogen peroxide (H_2O_2) can inflict damage to biomolecules under oxidative stress and also act as signaling molecules at physiological levels. Here we developed a unique chemical tool to elucidate the biological roles of ROS using both fluorescence imaging and conditional proteomics. H_2O_2-responsive protein labeling reagents (Hyp-L) were designed to selectively tag proteins under the oxidative conditions in living cells and tissues. The Hyp-L signal remained even after sample fixation, which was compatible with conventional immunostaining. Moreover, Hyp-L allowed proteomic profiling of the labeled proteins using a conditional proteomics workflow. The integrative analysis enabled the identification of ROS generation and/or accumulation sites with a subcellular resolution. For the first time, we characterized that autophagosomes were enriched with H_2O_2 in activated macrophages. Hyp-L was further applied to mouse brain tissues and clearly revealed oxidative stress within mitochondria by the conditional proteomics.

Introduction

Reactive oxygen species (ROS) are a class of oxygen-containing and reactive molecules that are produced in a wide range of biological processes.[1] They are often produced during oxidative stress and can damage lipids, proteins, and DNA, which contributes to aging and many human diseases, including cancer, inflammation, cardiovascular and neurodegenerative diseases.[2-5] Evidence also shows that ROS are generated as a normal byproduct of metabolism and at physiological levels, can regulate various signaling pathways.[6-9] In particular, hydrogen peroxide (H_2O_2) exhibits mild reactivity and is relatively stable,[1] making it an ideal signaling molecule that can diffuse and travel appreciable distances, while reversibly modifying critical cysteine thiols for redox signaling.[6,10] H_2O_2 production in various cell types has been shown to mediate diverse physiological processes, ranging from the immune response to growth factor stimulation.[11-14]

Fluorescent sensors that can detect ROS production in living systems are useful tools to understand their biological functions,[10,15-19] as exemplified by the boronate-based probes for the detection of H_2O_2.[10,15] When coupled with fluorescence microscopy, the localization of ROS production in living systems can be visualized. However, such sensors could readily migrate after ROS sensing by diffusion, which may lead to an inaccurate readout of ROS localization. Moreover, most fluorescent sensors are not amenable to fixation. Very recently, Chang and co-workers described a histochemical approach to detect H_2O_2 in fixed samples based on puromycin staining;[20] but their method did not provide subcellular resolution of H_2O_2 production. In addition to these imaging-based methods, redox proteomics that identify the oxidatively modified proteins is a complementary approach for elucidating the biological roles of ROS.[21-26] Despite these advanced technologies, a robust chemical tool capable of integrating multiple

approaches does not exist, yet is highly desirable for a more comprehensive view of ROS homeostasis.

Here we developed a unique chemical probe that allows for both fluorescence imaging and profiling of proteins under oxidative conditions in living cells and tissues. We designed H_2O_2-responsive labeling reagents named 'Hyp-L' that can be activated in the presence of H_2O_2 to covalently tag nearby proteins, producing an immobilized signal compatible with cell/tissue fixation and subsequent immunostaining. Furthermore, the proteins labeled with Hyp-L can be enriched and identified using a conditional proteomics workflow (Fig. 1a).[27,28] Integrated analysis by the Hyp-L-based protein labeling, imaging, and proteomics, together with the H_2O_2 imaging by a fluorescent sensor (HYDROP), enabled us to identify autophagosomes as H_2O_2-rich vesicular organelles in the activated RAW264.7 macrophages, as well as phagosomes, endosomes, and lysosomes. We further demonstrated that Hyp-L can be applied to mouse brain tissues, and the conditional proteomics clearly indicated mitochondrial ROS production upon inhibition of mitochondrial respiration in hippocampal slices.

Results

Design of Hyp-L

Hyp-L utilizes pinacolboronate as an H_2O_2-responsive group,[10,15] though it is known to also react with other ROS, e.g., $ONOO^-$,[29] for the selective activation under the oxidative conditions in living systems. The H_2O_2-mediated boronate oxidation reaction can produce a 2-fluoromethylphenol intermediate, which undergoes 1,4-elimination to generate a highly electrophilic quinone methide (QM)[30-32] for covalently labeling surrounding proteins. On the basis of Fick's law using the calculated half-life of QM, the diffusion radius of the Hyp-L-

generated QM was estimated to be less than 1 μm in solutions (see the estimation method in the Supporting Information). Given the crowded microenvironment and the membrane structures in living cells, the labeling by Hyp-L could be confined within the membrane-enclosed ROS-rich organelles.[33] Two types of Hyp-L, Hyp-L-1 and Hyp-L-2, were prepared by tethering coumarin and diacetyl fluorescein, respectively, for fluorescent imaging and/or affinity tagging of the labeled proteins.

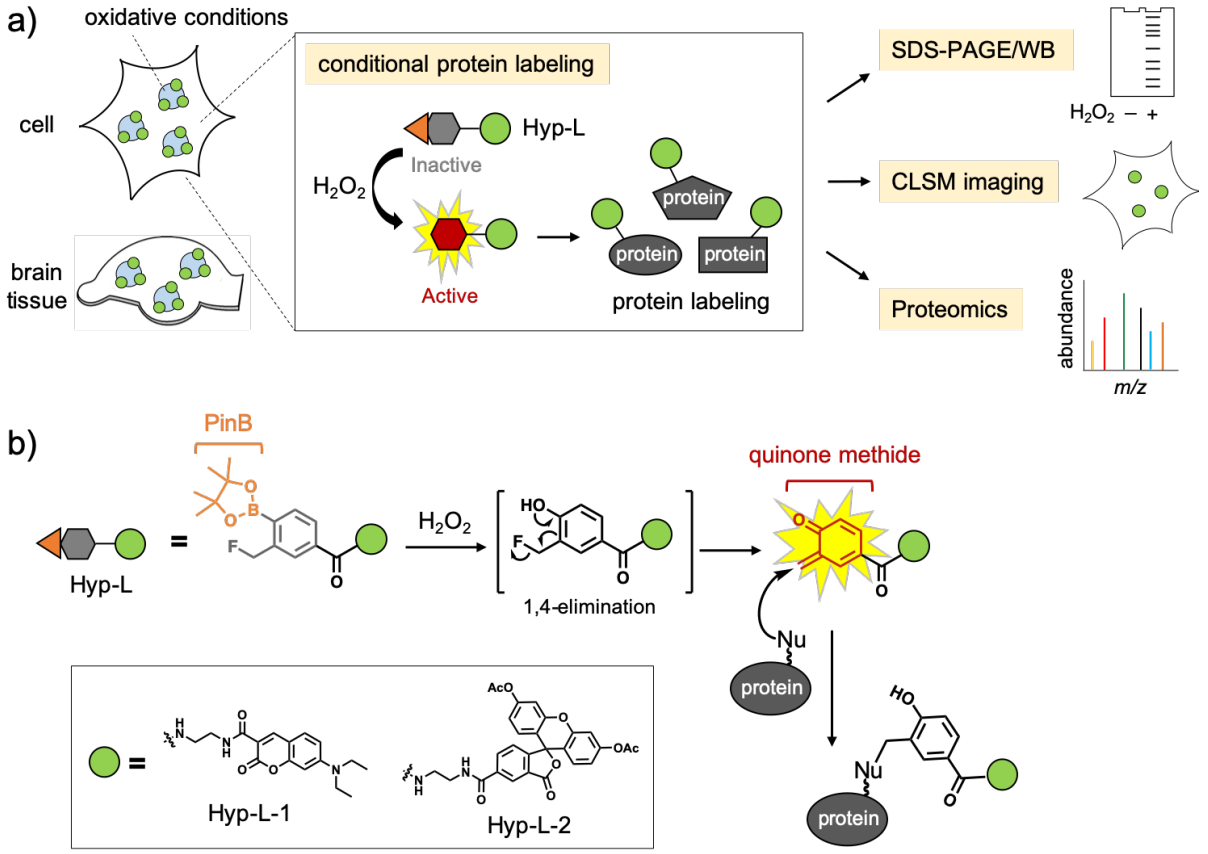

Figure 1 a) Illustration of Hyp-L-based conditional protein labeling for profiling and imaging of proteins under the oxidative conditions in cells and tissues. b) Schematic of H_2O_2-responsive protein labeling by Hyp-L. WB: western blot, Nu: nucleophilic amino acid, PinB: pinacolboronate.

H_2O_2-modulated reactivity of Hyp-L

The reactivity of Hyp-L-1 to H_2O_2 was evaluated by HPLC. Upon the addition of H_2O_2, Hyp-L-1 and its boronic-acid (BA) derivative (pinacolboronate was partially decomposed to BA during HPLC[34]) were rapidly consumed (Fig. 2a and Supplementary Fig. 1). Simultaneously, a hydroxymethylphenol derivative, the hydrolyzed product of QM, was newly generated as a major product with a recovery yield of ~80% after 30 min. A dimer formed by conjugation of one QM with one hydrolyzed QM was also detected with a quite low yield, suggesting the self-labeling of Hyp-L-1 was neglected. The H_2O_2-modulated hydrolysis proceeded in a dose-dependent manner (Supplementary Fig. 2).

The H_2O_2-responsive protein labeling was then examined using bovine serum albumin (BSA) as a model substrate *in vitro*. H_2O_2 was added to a solution of BSA containing Hyp-L-1, and the reaction was analyzed by SDS-PAGE and in-gel fluorescence imaging. The fluorescent BSA band appeared at 2 min and its intensity increased until 30 min (Supplementary Fig. 3a). A dramatic increase in BSA labeling was elicited by 50 μM of H_2O_2 (1 eq. to Hyp-L-1) (Supplementary Fig. 3b). By contrast, no fluorescent bands appeared in the absence of H_2O_2, clearly indicating that H_2O_2-responsive BSA labeling had occurred. We also confirmed that Hyp-L-1 was moderately selective for H_2O_2 compared with other ROS and reactive nitrogen species (RNS), including O_2^{-}, $^1O_2$, ·OH, ClO^{-}, and ·NO, except for $ONOO^{-}$ which was also able to trigger the BSA labeling (Fig. 2b and 2c). The labeling occurred at physiological pH, and the rate was moderately enhanced under basic conditions (between pH 6.0–8.0, see Supplementary Fig. 3c), likely due to the increased reactivity of nucleophilic amino acids of BSA upon deprotonation at basic pH.

The labeled amino acids were then identified by a conventional peptide mapping protocol, which included protein digestion and LC-MS/MS analysis. Eight types of nucleophilic amino acids were modified with Hyp-L-1, including His, Lys, Cys, Glu, Tyr, Ser, Thr, and Asp, whereas less reactive amino acids, such as Gly, were not labeled (Fig. 2d, Supplementary Fig. 4 and Fig. 5, and Supplementary Data 1). The labeled residues were primarily positioned and broadly distributed on the surface of BSA. This result revealed the high reactivity and wide amino acid coverage of the Hyp-L-generated QM.

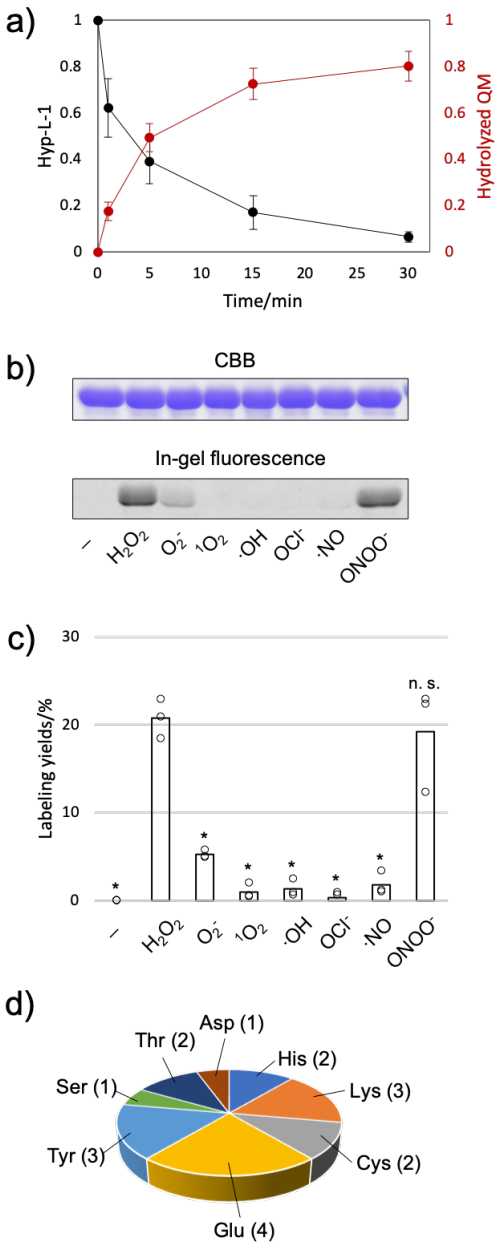

Figure 2 Activation of Hyp-L-1 by H_2O_2. a) Time course of hydrolysis in the presence of H_2O_2. 50 μM of Hyp-L-1 was incubated with 500 μM of H_2O_2 in PBS (−). The percentages of Hyp-L-1 and hydrolyzed QM were calculated according to the HPLC peak areas in Supplementary Fig. 1. Error bar indicates s.d., n = 3. b) ROS selectivity in BSA labeling. 200 μM of various ROS was added to a PBS (−) solution of BSA (10 μM) containing 50 μM of Hyp-L-1, and the mixture was incubated for 30 min. The upper panel shows a Coomassie Brilliant Blue (CBB) stained gel

image. c) Quantification of the labeling in b). The labeling yields were calculated based on the in-gel fluorescence intensities of Hyp-L-1-labeled BSA and a standard Dc-BSA (see the calculation method in the Supporting Information). Statistical analyses were performed with a two-tailed Student's *t*-test ($n = 3$) relative to the data of H_2O_2-induced labeling. *$P < 0.05$, n.s.: not statistically significant. d) Hyp-L-1-modified amino acid residues on BSA.

H_2O_2-responsive labeling in living cells

For the labeling in living cells, we used Hyp-L-2 bearing diacetyl fluorescein as a reporter, because i) the fluorescein dye emits at a longer wavelength than coumarin, ii) its antibody is available with a high and specific affinity, and iii) masking with two acetyl groups, which can be readily cleaved by intracellular esterases, greatly improves cell permeability. RAW264.7 macrophage was selected as a cell line for H_2O_2-mediated immune response assays.[16,35,36] CLSM imaging showed that Hyp-L-2 could be rapidly taken up by living cells within 5 min, and bright intracellular fluorescence was broadly distributed across the entire cell (Supplementary Fig. 6), which is preferable for unbiased intracellular protein labeling. Hyp-L-2 showed low cytotoxicity after the incubation for 1 h (Supplementary Fig. 7). The H_2O_2-responsive labeling of Hyp-L-2 in living cells was initially tested by adding exogenous H_2O_2. In the presence of H_2O_2, multiple fluorescent bands over a wide molecular weight range were clearly detected by in-gel fluorescence imaging. However, in the absence of H_2O_2, no significant signals were observed (Fig. 3a and 3b). The increased fluorescence bands were detectable at 10 μM H_2O_2, suggesting sufficient sensitivity of Hyp-L-2 to physiological levels of H_2O_2.[8,9] The labeled proteins could be directly visualized by CLSM imaging in fixed cells, revealing that the fluorescein-tagged proteins were intracellularly localized with an unbiased distribution (Fig. 3c). By contrast, non-

H_2O_2-treated cells became relatively dark after cell fixation, because the small molecules of unreacted Hyp-L-2 could be easily washed out. As a control, we used HYDROP, a commercially available fluorescent H_2O_2 sensor. Its fluorescence clearly increased upon H_2O_2 addition in living cells (Supplementary Fig. 8) but was extinguished after cell fixation (Fig. 3d). This highlighted a key advantage of Hyp-L-2 over conventional H_2O_2 sensors for fixed-cell imaging.

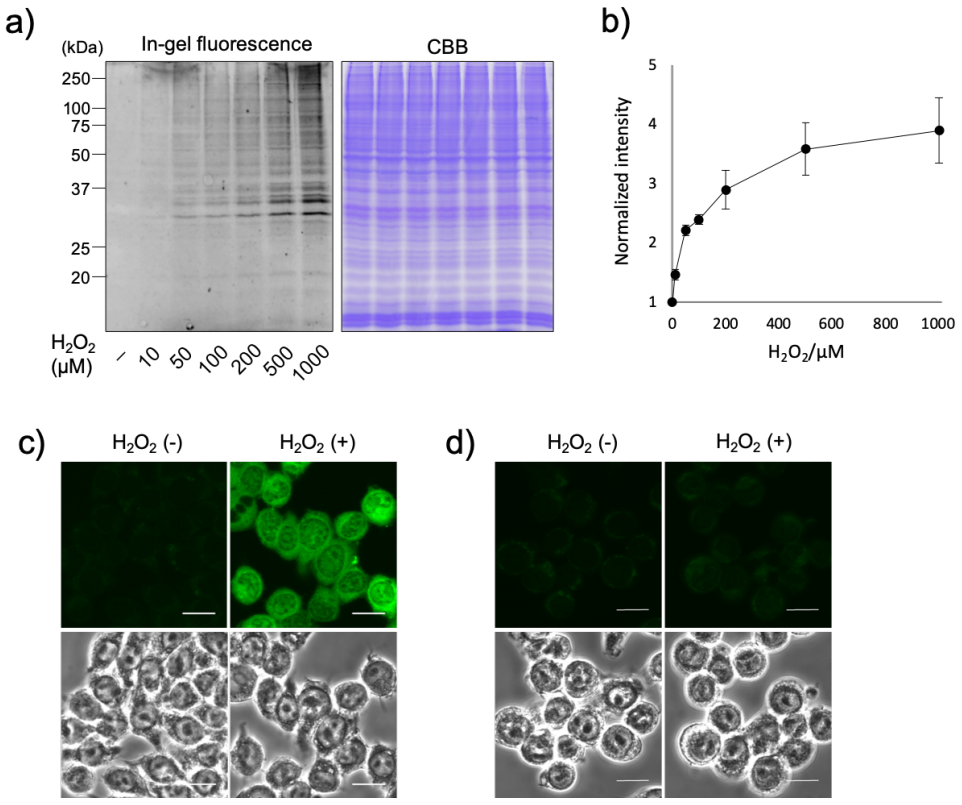

Figure 3 H_2O_2-responsive protein labeling by Hyp-L-2 in living RAW264.7 macrophages. a) SDS-PAGE analysis. Cells were treated with 5 μM of Hyp-L-2 for 10 min, followed by incubation with a varied concentration of H_2O_2 for 30 min. b) Quantification of the labeling in a). The band intensities were normalized to the data of H_2O_2 (–). Error bar indicates s.d., n = 3. CLSM imaging of the fixed cells after the labeling by Hyp-L-2 (c) and HYDROP (d). H_2O_2: 100 μM. The cells were fixed with chilled methanol. Scale bars, 10 μm.

Conditional protein labeling in PMA-activated macrophages

We next tested Hyp-L-2 in the conditional protein labeling upon physiological stimulation. Professional phagocytes, such as macrophages, produce ROS during immune response when phagocytosis of microbes or encountering non-particulate stimuli. Phorbol myristate acetate (PMA) is one such stimulus and mimics the signal transduction pathway that assembles NADPH oxidase (NOX).[36-39] Diverse ROS-rich vesicles have been discovered in PMA-treated RAW264.7 macrophages by fluorescence imaging using ROS sensors.[16,35] However, the exact nature of these ROS-producing/accumulated organelles has not yet been determined.[37-39] We thus attempted to address this by identifying proteins in the ROS-rich vesicles using the Hyp-L-based proteomics.

We initially evaluated the protein labeling by Hyp-L-2 in response to PMA stimulation in RAW264.7 macrophages. Cells were treated with PMA for 30 min, followed by incubation with Hyp-L-2 for another 30 min. Protein labeling was assessed by western blot using an anti-fluorescein antibody (Fig. 4a and 4b). The band intensity and the number of labeled proteins substantially increased upon the PMA stimulation, and this could be blocked by inhibition of NOX with diphenyleneiodonium (DPI) or apocynin. Ebselen, a mimic of the H_2O_2 scavenger glutathione peroxidase, and *N*-acetylcysteine (NAC), a frequently used antioxidant, also significantly quenched the labeling. L-NAME can inhibit the production of ·NO by nitric oxide synthase (NOS) and the subsequent conversion of ·NO to $ONOO^-$. We found that L-NAME had little effect on the protein labeling and the expression of inducible NOS (iNOS) kept minimal upon the PMA stimulation (Supplementary Fig. 9). These results indicate that the endogenously produced H_2O_2 could be mainly responsible for the enhanced protein labeling by Hyp-L-2 in PMA-stimulated macrophages. By contrast, a bromo analogue of Hyp-L-2, compound 8, lacking

the H_2O_2-sensitive boronate group, was unable to produce any protein labeling signals regardless of the PMA stimulation (Supplementary Fig. 10).

We next visualized the labeled proteins by CLSM imaging after the cell fixation. Strong and punctate fluorescence from vesicles was observed in the PMA-treated cells, whereas the untreated control cells showed negligible fluorescence (Fig. 4c). Notably, PMA did not affect the cellular uptake of Hyp-L-2 (Fig. 4d). This might suggest that the elevated intracellular H_2O_2 was likely enclosed within the vesicular organelles. The punctate fluorescence was abolished by the treatment with DPI, apocynin, ebselen, and NAC, but not affected by L-NAME (Supplementary Fig. 11), which was consistent with the above western blot data (Fig. 4a and 4b). We also observed similar vesicular imaging by HYDROP, which is specific to H_2O_2, in the PMA-activated living cells (Supplementary Fig. 12).

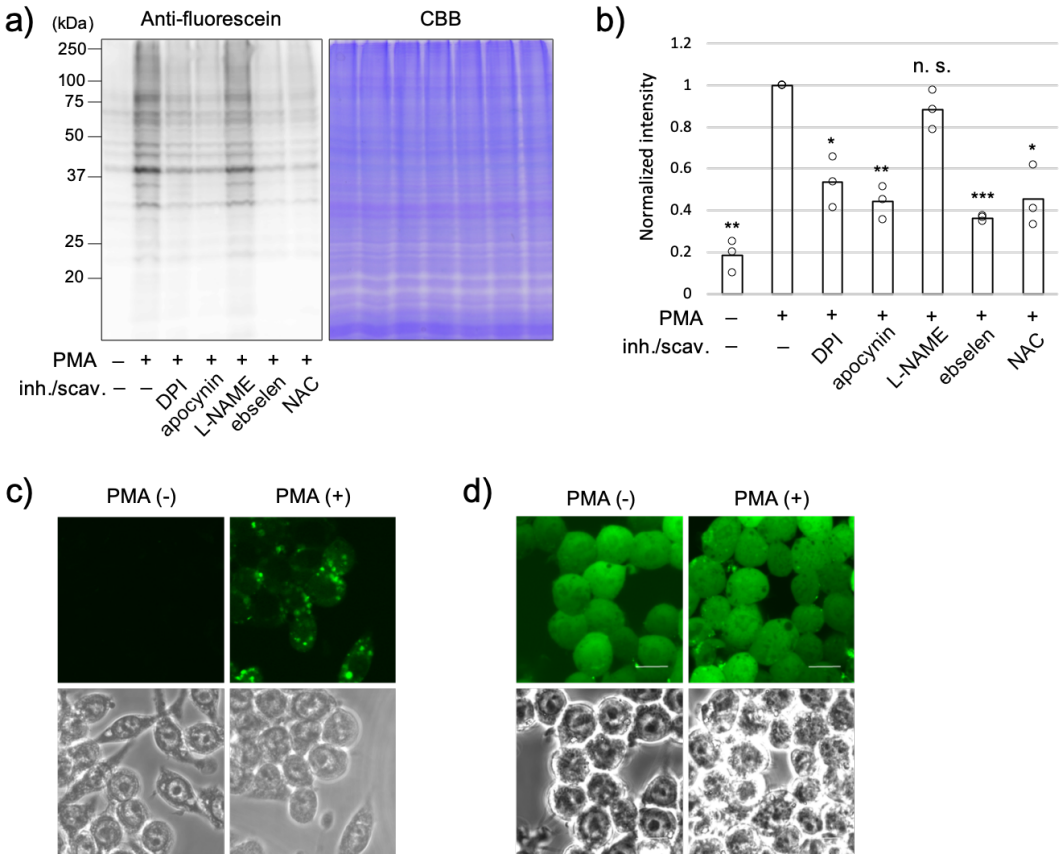

Figure 4 Conditional protein labeling in RAW264.7 macrophages upon PMA stimulation. a) Western blot analysis. RAW264.7 macrophages were activated with 1 μg/mL of PMA in the absence or presence of various inhibitors or scavengers for 30 min, followed by incubation with 5 μM of Hyp-L-2 for 30 min. After cell lysis and SDS-PAGE, the labeled proteins were detected by western blot using an anti-fluorescein antibody. DPI: 10 μM, apocynin: 5 mM, L-NAME: 5 mM, ebselen: 5 μM, NAC: 10 mM. b) Quantification of the labeling in a). The band intensities were normalized to the data of PMA (+). Statistical analyses were performed with a two-tailed Student's *t*-test ($n = 3$) relative to the data of PMA (+). *$P < 0.05$, **$P < 0.01$, ***$P < 0.01$, n.s.: not statistically significant. CLSM imaging of the fixed (c) and living (d) cells labeled by Hyp-L-2. After the PMA stimulation as a), the cells were incubated with Hyp-L-2 for 30 min (c) or 10 min (d). The cells were fixed with chilled methanol in c) before imaging. Scale bars: 10 μm.

Proteomic profiling and vesicle identification

To identify proteins associated with the H_2O_2 produced upon PMA stimulation, we coupled the labeling by Hyp-L-2 with LC-MS/MS analysis (Fig. 5a). The labeled proteins were enriched by immunoprecipitation (IP) (Fig. 5b) and in-gel digested by trypsin. We carried out quantitative mass analysis using tandem mass tagging (TMT). The digested peptides were tagged by heavy (H) and light (L) TMT reagents for PMA (+) and PMA (−) samples, respectively, which were then mixed in a 1:1 ratio and subjected to LC-MS/MS analysis.

A total of 171 proteins were identified, among which 170 (> 99%) proteins showed above zero values in log2 fold change (H/L ratio), indicating that the protein labeling by Hyp-L-2 was indeed strongly affected by PMA stimulation (Fig. 5c and Supplementary Data 2). Six proteins, such as Eif4a1, Rab5c, and Pfn1, were only labeled in PMA-treated macrophages with a maximal H/L ratio of 100, and 63 proteins were significantly enriched ($\log_2(H/L) > 1$) with high fidelity ($P < 0.05$).[40] These 69 promising protein candidates were categorized into group A for further analysis.

To characterize the labeled proteins in group A, we performed gene ontology (GO) enrichment analysis. The cellular component analysis showed that vesicular proteins were significantly enriched (Fig. 5d), consistent with the punctate signals in our fixed-cell imaging. We also conducted western blot analysis of several highly-enriched proteins in group A (Supplementary Fig. 14), as well as DNA microarray analysis for the whole transcriptome in RAW264.7 macrophages (Supplementary Fig. 15 and 16). These results indicated that expression at both the protein and mRNA levels did not change significantly before and after the PMA stimulation. Thus, the proteomic profiling most likely reflected responsive protein labeling in the H_2O_2-rich compartments, rather than changes in protein expressions.

We next attempted to identify the H_2O_2-rich vesicles based on the proteomics results. Several proteins in group A could be assigned to specific vesicular organelles, including phagosomes, endosomes, and lysosomes (Supplementary Table 1). This is consistent with the previous reports that phagosomes and endosomes recruit NOX on their membranes and enrich ROS during the immune response.[1,38,39,41] Also, it is known that overproduced H_2O_2 can diffuse into lysosomes.[42] The HYDROP-stained vesicles in PMA-treated living cells indeed moderately colocalized with LysoTracker Deep Red (LysoDR, Supplementary Fig. 17), a fluorescent dye for staining acidic organelles, such as lysosomes and endosomes. We also noticed that GO enrichment analysis of proteins in group A characterized intracellular compartments other than vesicles, such as ribosomes and mitochondria (Fig. 5d). We selected two mitochondrial proteins in group A, Sdha (H/L ratio = 3.39) and Hspa9 (H/L ratio = 2.77), for immunostaining after the conditional labeling by Hyp-L-2. The antibodies were validated by siRNA knockdown (Supplementary Fig. 18 and Fig. 19). Sdha and Hspa9 showed punctate signals in the PMA-activated macrophages, which could be partially merged with the Hyp-L-2-labeled vesicles (Fig. 5e and Supplementary Fig. 20). Given previous studies,[43,44] these might be caused by a self-engulfing process inside cells *via* PMA-induced autophagy. We therefore hypothesized that H_2O_2 was also enriched within autophagosomes. Indeed, HYDROP was partially colocalized with mCherry-LC3B, a standard autophagosome marker (Fig. 5f and Supplementary Fig. 23). Taken together, we concluded that the H_2O_2 generated upon PMA stimulation in RAW264.7 macrophages was likely enriched within a wide range of vesicular organelles, including phagosomes, endosomes, lysosomes, and autophagosomes.

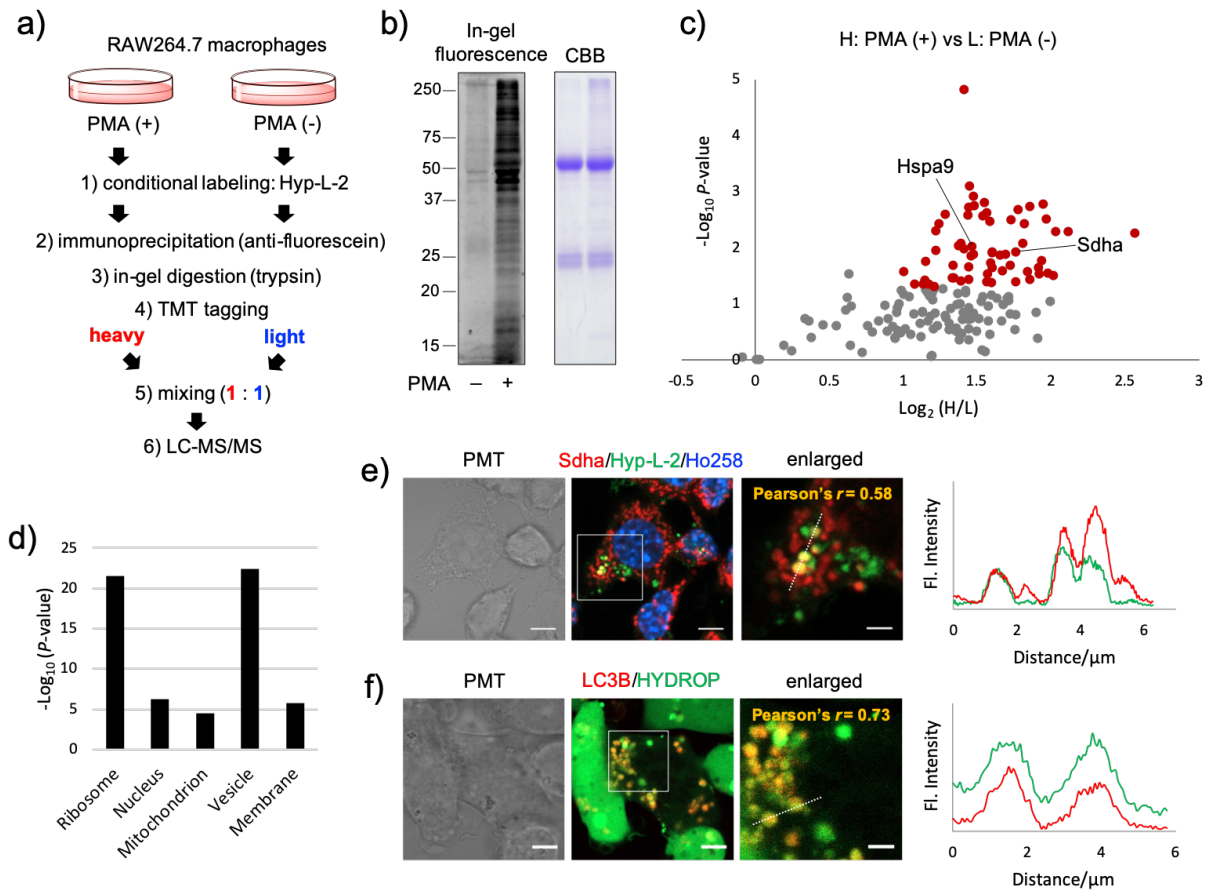

Figure 5 Proteomic analysis of the labeled proteins in RAW264.7 macrophages. a) Workflow for TMT-based quantitative proteomic analysis of PMA (+) vs PMA (–). b) In-gel fluorescence imaging of IP-enriched proteins. c) Volcano plot obtained by the *P*-value of H: PMA (+) vs L: PMA (–) against Log_2 (H/L). The proteins showing log_2 (H/L) > 1.0 and $P < 0.05$ were highlighted in red. *P*-value was calculated by the Benjamini–Hochberg procedure. Six proteins only labeled in the PMA (+) sample were not plotted, including Eif4a1, Rab5c, Pcbp1, Pfn1, Ppl27a, and Lmnb1. Two proteins analyzed by immunostaining were denoted. d) GO enrichment analysis of the 69 proteins in group A (64 protein IDs were mapped). e) Representative CLSM imaging of the immunofluorescence against Sdha that were partially merged with Hyp-L-2-labeled vesicles in PMA-stimulated RAW264.7 macrophages. The nucleus was stained with

Hoechst 33258 (Ho258). The antibody was validated by siRNA knockdown (Supplementary Fig. 18 and Fig. 19). f) Representative CLSM imaging of mCherry-LC3B with HYDROP in PMA-stimulated RAW264.7 macrophages. Images from 4 separate fields containing over 10 cells were collected and analyzed for e) and f). See Supplementary Fig. 20 and Fig. 23 for images in other fields. Line-plot graphs indicate the fluorescence intensity profiles of Sdha or LC3B (red) and Hyp-L-2 (green) along the white dotted lines. Colocalization was quantified using Pearson's *r*. Scale bars, 5 µm and 2 µm (enlarged images).

Conditional protein labeling under mitochondrial oxidative stress

Hyp-L-2 is applicable for the conditional protein labeling within other cellular compartments. Mitochondrial respiratory chain is the main producer of cellular energy and is also a major source of ROS in mammalian cells. Disorder of the mitochondrial respiratory chain complexes may therefore promote the overproduction of ROS. We used 2-thenoyltrifluoroacetone (TTFA), a mitochondrial complex II inhibitor that binds to the ubiquinone-binding site, to induce oxidative stress within mitochondria in HeLa cells.[45,46] SDS-PAGE analysis showed increased protein labeling by Hyp-L-2 in response to the TTFA stimulation (Fig. 6a and 6b). To determine the subcellular localization of the labeled proteins, HeLa cells were stained with MitoTracker Deep Red (MitoDR) prior to the treatment with TTFA and labeling by Hyp-L-2. MitoDR contains a thiol-reactive chloromethyl moiety for mitochondrial labeling, that allows imaging of fixed cells. Although Hyp-L-2 inside living cells treated with TTFA was homogenously distributed throughout the cell, the retained Hyp-L-2 fluorescence after cell fixation was heterogeneous (Fig. 6c) and merged well with MitoDR (Fig. 6d). This gave us additional evidence that the Hyp-L-based conditional labeling was able to address the ROS production with

a subcellular resolution. Interestingly, we observed TTFA-induced fragmentation of mitochondria into punctate vesicles (Supplementary Fig. 24), which is consistent with the previous report that inhibition of mitochondrial respiratory chain causes ROS-mediated autophagy.[46]

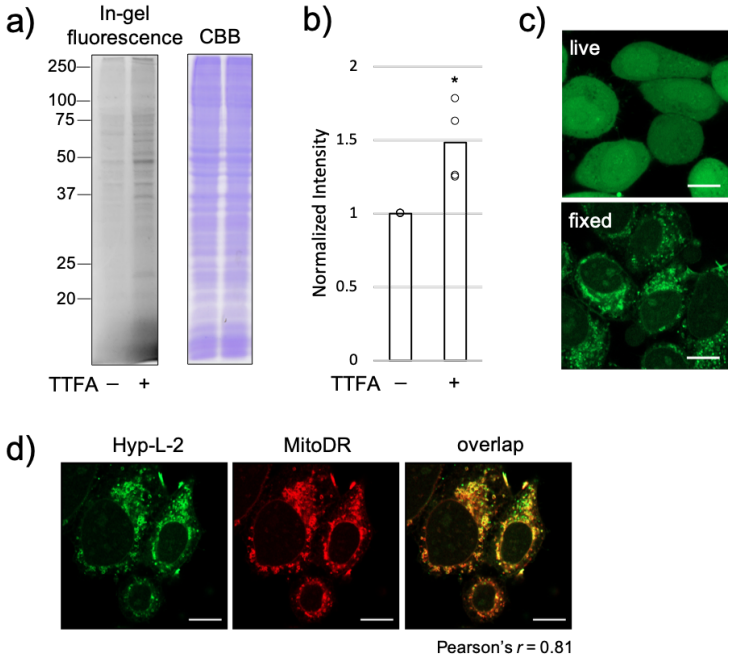

Figure 6 Conditional protein labeling under mitochondrial oxidative stress in HeLa cells. a) SDS-PAGE analysis of TTFA-induced labeling. HeLa cells were treated with 1 mM of TTFA for 30 min, followed by incubation with 5 μM of Hyp-L-2 for 30 min. b) Quantification of the labeling in a). The band intensities were normalized to the data of TTFA (–). Statistical analyses were performed with a two-tailed Student's *t*-test ($n = 4$) relative to the data of TTFA (–). $^{**}P < 0.01$. c) CLSM imaging of TTFA-treated cells. After the labeling as a), cells were subjected to CLSM imaging before (upper) and after (lower) the fixation with chilled methanol. d) Colocalization imaging of Hyp-L-2 with MitoDR in TTFA-treated cells. HeLa cells were stained with 200 nM of MitoDR before the TTFA stimulation and the Hyp-L-2 labeling. The cells were

fixed with chilled methanol before CLSM imaging. Colocalization was quantified using Pearson's *r*. Scale bars, 10 μm.

Application of Hyp-L to mouse brain tissue

The brain is a metabolically active organ exhibiting a high demand for energy and oxygen, together with robust ROS production. Abnormally high levels of ROS in the brain lead to neuronal toxicity and neurodegeneration,[3] on the other hand, ROS at physiological concentrations are involved in synaptic plasticity.[47,48] We further explored the applicability of Hyp-L in mouse brain tissues. Acute hippocampal slices (250 μm thick) were prepared and incubated with Hyp-L-2 in artificial cerebrospinal fluid (ACSF) for 60 min, followed by treatment with 1 mM of H_2O_2 for 30 min and tissue fixation. An increase in the fluorescent signal in response to H_2O_2 was clearly observed by fixed-tissue imaging (Supplementary Fig. 25a). Z-axis scanning of the labeled slices revealed efficient tissue penetration of Hyp-L-2 to a depth of ~100 μm (Supplementary Fig. 25b). Western blot analysis confirmed the H_2O_2-induced protein labeling by Hyp-L-2 in the tissues (Supplementary Fig. 26).

Conditional protein labeling in brain tissue was demonstrated under the oxidative stress induced by TTFA. SDS-PAGE analysis showed significantly increased fluorescent bands in hippocampal slices treated with TTFA, which was suppressed by ebselen or skQ1, a mitochondrial antioxidant (Fig. 7a and 7b). CLSM imaging with HYDROP in living slices verified the increased H_2O_2 production induced by TTFA (Supplementary Fig. 27). However, such fluorescence signals were completely abolished after tissue fixation (Fig. 7c). By contrast, TTFA-induced labeling by Hyp-L-2 remained fluorescent in the fixed slices (Fig. 7d and 7e). We subsequently attempted to investigate whether the conditional labeling indeed occurred within

mitochondria *via* colocalization imaging by using MitoDR and anti-Sdha, a mitochondrial antibody marker. After fixation and permeabilization, the slices were further trimmed to 40 μm to improve antibody penetration. Unfortunately, the CLSM imaging results were ambiguous (Supplementary Fig. 28), because the complex tissue structure made it difficult to distinctly recognize mitochondria, unlike that in simple cultured cells.

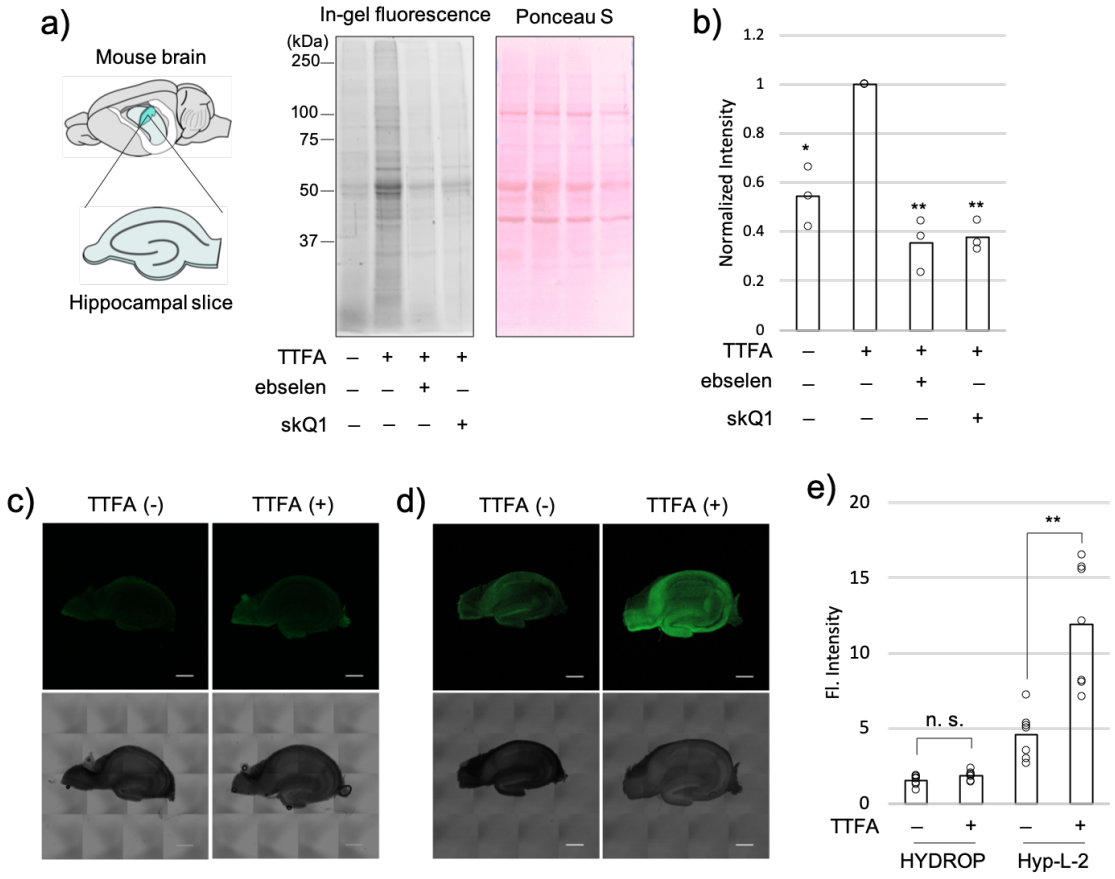

Figure 7 Application of Hyp-L-2 to mouse brain tissues. a) SDS-PAGE analysis of the conditional protein labeling upon TTFA stimulation. Acutely prepared slices were treated with 1 mM of TTFA in the absence or presence of ebselen or skQ1 (10 μM) for 30 min, followed by incubation with 5 μM of Hyp-L-2 for 60 min. The right panel shows an image of the Ponceau S stained PVDF membrane. b) Quantification of the labeling in a). The band intensities were

normalized to the data of TTFA (+). Statistical analyses were performed with a two-tailed Student's *t*-test ($n = 3$) relative to the data of TTFA (+). *$P < 0.05$, **$P < 0.01$. CLSM imaging of hippocampal slices labeled by HYDROP (c) and Hyp-L-2 (d) in response to the TTFA stimulation. After the labeling as a), slices were fixed, permeabilized, and subjected to CLSM imaging. Scale bars, 500 μm. e) Quantification of the labeling in c) and d). The fluorescence intensities were extracted from seven POIs in each image of c) and d). Statistical analyses were performed with a two-tailed Student's *t*-test ($n = 7$) relative to the data of TTFA (–). **$P < 0.01$, n.s.: not statistically significant.

As demonstrated above, proteomics data are complementary to imaging experiments by providing valuable information about the subcellular sources of ROS. We thus used TMT-based quantitative proteomics to clarify the localization of the labeled proteins (Fig. 8a). A total of 253 proteins were identified, which included 252 proteins showing above zero log2 fold change (H: TTFA (+)/ L: TTFA (−)) values (Fig. 8c and Supplementary Data 4). 130 proteins that were highly and significantly enriched ($\log_2(H/L) > 1$, $P < 0.05$) were categorized into group B and subjected to GO enrichment analysis. The cellular component analysis revealed that the labeled proteins were selectively and significantly enriched in mitochondria, while some proteins were moderately enriched in the cytosol and cytoskeleton (Fig. 8d). Biological process analysis significantly characterized ROS- and mitochondria-associated processes, such as ROS metabolic processes and electron transport chain (Fig. 8e), in good agreement with the cellular component analysis. The proteins in group B were also individually analyzed with Uniprot, identifying 35 mitochondrial proteins, including 8 proteins assigned to the mitochondrial respiratory chain (Supplementary Data 4). In particular, 7 of the top 10 proteins in group B were annotated as

mitochondrial proteins (Fig. 8c). These results clearly demonstrated that the Hyp-L-based conditional proteomics worked well even in tissue samples and that TTFA indeed pharmacologically enhanced ROS production in mitochondria of hippocampal slices.

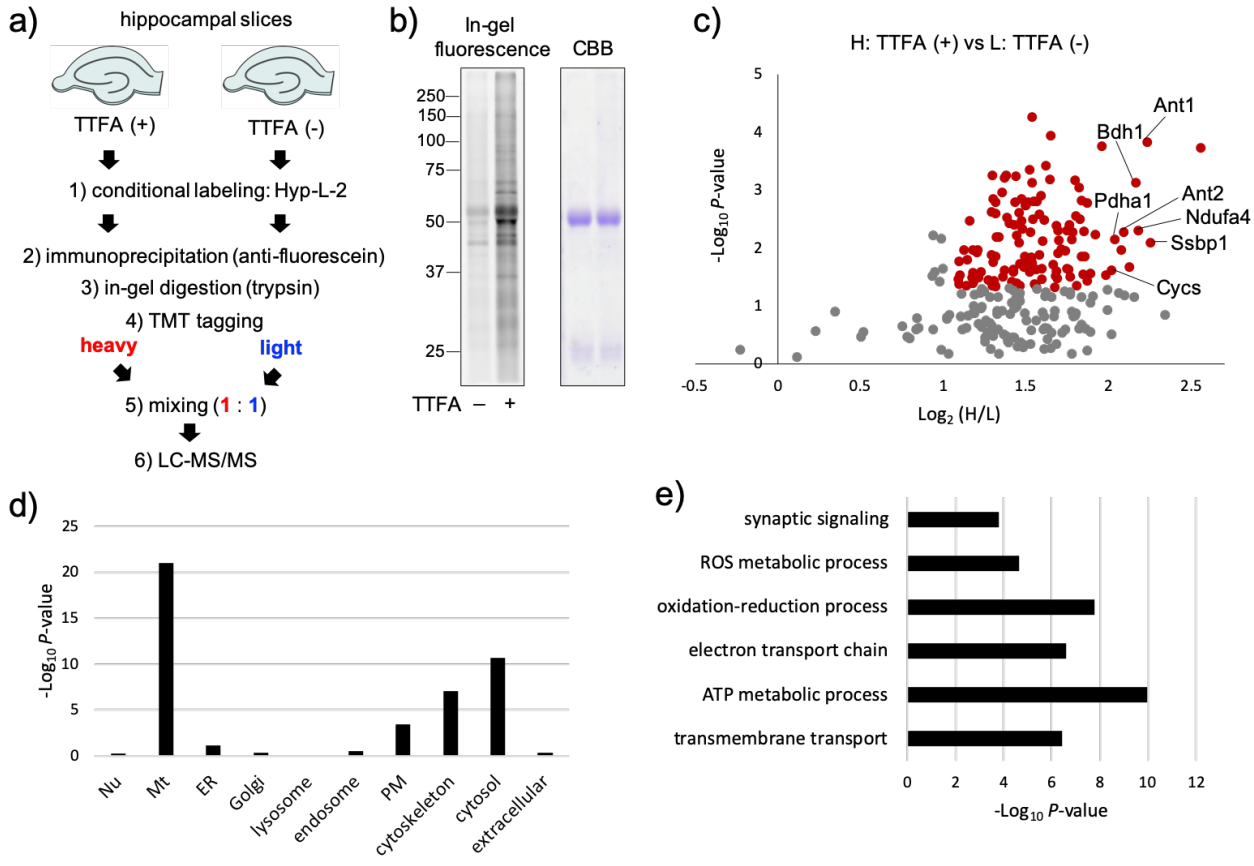

Figure 8 Proteomic analysis of the labeled proteins in hippocampal slices. a) Workflow for TMT-based quantitative proteomic analysis of TTFA (+) vs TTFA (−). b) In-gel fluorescence imaging of IP-enriched proteins. c) Volcano plot obtained by the *P*-value of H: TTFA (+) vs L: TTFA (−) against Log_2 (H/L). The proteins showing log_2 (H/L) > 1.0 and $P < 0.05$ are highlighted in red. *P*-value was calculated by the Benjamini−Hochberg procedure. Seven of the top 10 proteins in group B that assigned to mitochondria were denoted. d) Cellular component

and e) biological process analysis of the 130 proteins in group B (111 protein IDs were mapped). Nu: nucleus, Mt: mitochondrion, ER: endoplasmic reticulum, PM: plasma membrane.

Discussion

We have developed a new chemical probe, Hyp-L, which relies on H_2O_2-induced covalent protein labeling in live cells, for both fluorescence imaging and profiling of proteins under the oxidative conditions. It was further demonstrated that the Hyp-L-based conditional proteomics was able to identify oxidative stress with a subcellular resolution in tissue specimens, which remains challenging for imaging with the conventional H_2O_2 sensors due to the complex structure and cell-type heterogeneity of tissues.

Although useful, it is noteworthy to point out the (potential) limitations and drawbacks of Hyp-L, including (i) the moderate ROS selectivity, (ii) the relatively large diffusion radius, (iii) the pH dependence on the labeling reaction, (iv) the potential competition and/or consumption by cellular antioxidants, (v) potentially biased protein labeling due to the limited amino acid coverage and/or interactions with some specific proteins. Given these, one should carefully design the experiments and analyze/validate the results provided by Hyp-L. For instance, inhibitory assays for ROS/RNS generation enzymes may determine whether the conditional labeling by Hyp-L is due to H_2O_2. The production and distribution of H_2O_2 can be validated by the imaging with some H_2O_2-selective sensors.[16,18] Also, characterizing proteins that may localize in subcellular compartments of acidic pH and/or rich cellular antioxidants must be conducted with great attention.

Indeed, such integrative analysis that was triggered with experiments of Hyp-L provided a wealth of data regarding the subcellularly resolved ROS homeostasis as shown here. We

identified, for the first time, that autophagosomes contained a high level of H_2O_2 in the activated macrophages. Our results provide direct evidence of the linkage between H_2O_2 homeostasis and autophagy,[49] which will be valuable for elucidating the mechanism underlying the ROS-induced autophagy in immunity.[50]

We envision the future use of Hyp-L to unravel important, yet to be clearly addressed, issues regarding ROS roles in diverse physiological and pathological processes, such as NMDR receptor-mediated signaling,[48] inflammation, and ischemia-reperfusion injury.[4] For these directions, the further improvement of probe molecules is keenly required in several issues including the points mentioned above, as well as the development of various chemical probes showing distinct ROS selectivity.

Supporting information

Supplementary figures and tables, experimental procedures, synthesis, and characterization of compounds; Supplementary Data 1-4.

Acknowledgments

We thank Dr. Shigeki Kiyonaka (Nagoya University) for support in brain slice experiments, Dr. Wataru Aoki (Kyoto University) for experimental support in the determination of labeling sites, and Dr. Takayuki Miki (Tokyo Institute of Technology) for discussions in probe design and proteomic analysis. We also thank Kathy Tamai in Edanz Group (www.edanzediting.com) for editing a draft of this manuscript. This work was funded by Grant-in-Aid for JSPS fellows (17F17344) to H.Z., Grant-in-Aid for Young Scientists (18K14334) and Grant-in-Aid for Scientific Research on Innovative Areas “Integrated Bio-metal Science” (19H05764) to T.T., and

Japan Science and Technology Agency (JST) ERATO Grant JPMJER1802 to I.H. This work was also supported by a Grant-in-Aid for Scientific Research on Innovative Areas "Chemistry for Multimolecular Crowding Biosystems" (17H06348) to I.H.

Competing financial interests

The authors declare no competing interests.

References

(1) Winterbourn, C. C. Reconciling the chemistry and biology of reactive oxygen species. *Nat. Chem. Biol.* **2008**, *4*, 278.

(2) Finkel, T.; Holbrook, N. J. Oxidants, oxidative stress and the biology of ageing. *Nature* **2000**, *408*, 239.

(3) Lin, M. T.; Beal, M. F. Mitochondrial dysfunction and oxidative stress in neurodegenerative diseases. *Nature* **2006**, *443*, 787.

(4) Valko, M.; Leibfritz, D.; Moncol, J.; Cronin, M.; Mazur, M.; Telser, J. Free radicals and antioxidants in normal physiological functions and human disease. *Int. J. Biochem. Cell Biol.* **2007**, *39*, 44.

(5) Kanvah, S.; Joseph, J.; Schuster, G. B.; Barnett, R. N.; Cleveland, C. L.; Landman, U. Oxidation of DNA: damage to nucleobases. *Acc. Chem. Res.* **2010**, *43*, 280.

(6) D'Autréaux, B.; Toledano, M. B. ROS as signaling molecules: mechanisms that generate specificity in ROS homeostasis. *Nat. Rev. Mol. Cell Biol.* **2007**, *8*, 813.

(7) Bedard, K.; Krause, K-H. The NOX family of ROS-generating NADPH oxidases: physiology and pathophysiology. *Physiol. Rev.* **2007**, *87*, 245.

(8) Dickinson, B. C.; Chang, C. J. Chemistry and biology of reactive oxygen species in signaling or stress responses. *Nat. Chem. Biol.* **2011**, *7*, 504.

(9) Murphy, M. P.; Homgren, A.; Larsson, N.; Halliwell, B.; Chang, C. J.; Kalyanaraman, B.; Rhee, S. G.; Thornalley, P. J.; Partridge, L.; Gems, D.; Nyström, T.; Belousov, V.; Schumacker, P. T.; Winterbourn, C. C. Unraveling the biological roles of reactive oxygen species. *Cell Metab.* **2011**, *13*, 361.

(10) Brewer, T. F.; Carcia, F. J.; Onak, C. S.; Carroll, K. S.; Chang, C. J. Chemical approaches to discovery and study of sources and targets of hydrogen peroxide redox signaling through NADPH oxidase proteins. *Annu. Rev. Biochem.* **2015**, *84*, 765.

(11) Babior, B. M.; Kipnes, R. S.; Curnutte, J. T. Biological defense mechanisms. The production by leukocytes of superoxide, a potential bactericidal agent. *J. Clin. Invest.* **1973**, *52*, 741.

(12) Sundaresan, M.; Yu, Z.; Ferrans, V. J.; Irani, K.; Finkel, T. Requirement for generation of H_2O_2 for platelet-derived growth factor signal transduction. *Science* **1995**, *270*, 296.

(13) Niethammer, P.; Grabher, C.; Look, A. T.; Mitchison, T. J. A tissue-scale gradient of hydrogen peroxide mediates rapid wound detection in zebrafish. *Nature* **2009**, *459*, 996.

(14) Dickinson, B. C.; Peltier, J.; Stone, D.; Schaffer, D. V.; Chang, C. J. Nox2 redox signaling maintains essential cell populations in the brain. *Nat. Chem. Biol.* **2011**, *7*, 106.

(15) Lippert, A. R.; Van de Bittner, G. C.; Chang, C. J. Boronate oxidation as a biorthogonal reaction approach for studying the chemistry of hydrogen peroxide in living systems. *Acc. Chem. Res.* **2011**, *44*, 793.

(16) Abo, M.; Urano, Y. Hanaoka, K.; Terai, T.; Komatsu, T.; Nagano, T. Development of a highly sensitive fluorescence probe for hydrogen peroxide. *J. Am. Chem. Soc.* **2011**, *133*, 10629.

(17) Dwyer, D. J.; Belenky, P. A.; Yang, J. H.; MacDonald, I. C.; Martell, J. D.; Takahashi, N.; Chan, C. T. Y.; Lobritz, M. A.; Braff, D.; Schwarz, E. G.; Ye, J. D.; Pati, M.; Vercruysse, M.; Ralifo, P. S.; Allison, K. R.; Khalil, A. S.; Ting, A. Y.; Walker, G. C.; Collins, J. J. Antibiotics induce redox-related physiological alterations as part of their lethality. *Proc. Natl. Acad. Sci.* **2014**, *111*, E2100.

(18) Ye, S.; Hu, J. J.; Yang, D. Tandem payne/dakin reaction: a new strategy for hydrogen peroxide detection and molecular imaging. *Angew. Chem. Int. Ed.* **2018**, *57*, 10173.

(19) Bai, X.; Ng, K. K.; Hu, J. J.; Ye, S.; Yang, D. Small-molecule-based fluorescent sensors for selective detection of reactive oxygen species in biological systems. *Annu. Rev. Biochem.* **2019**, *88*, 605.

(20) Chung, C. Y.; Timblin, G. A.; Saijo, K.; Chang, C. J. Versatile histochemical approach to detection of hydrogen peroxide in cells and tissues based on puromycin staining. *J. Am. Chem. Soc.* **2018**, *140*, 6109.

(21) Butterfield, D. A.; Boyd-Kimball, D. Redox proteomics and amyloid *ß*-peptide: insights into Alzheimer disease. *J. Neurochem.* **2019**, *151*, 459-487.

(22) Sultana, R.; Boyd-Kimball, D.; Poon, H. F.; Cai, J.; Pierce, W. M.; Klein, J. B.; Merchant, M.; Markesbery, W. R.; Butterfield, D. A. Redox proteomics identification of oxidized proteins in Alzheimer's disease hippocampus and cerebellum: an approach to understand pathological and biochemical alterations in AD. *Neurobiol. Aging* **2006**, *27*, 1564-1576.

(23) Yang, J.; Gupta, V.; Carroll, K. S.; Liebler, D. C. Site-specific mapping and quantification of protein S-sulphenylation in cells. *Nat. Commun.* **2014**, *5*, 4776.

(24) Akter, S.; Fu, L.; Jung, Y.; Conte, M-L.; Lawson, J. R.; Lowther, W. T.; Sun, R.; Liu, K.; Yang, J.; Carroll, K. S. Chemical proteomics reveals new targets of cysteine sulfinic acid reductase. *Nat. Chem. Biol.* **2018**, *14*, 995.

(25) Alcock, L. J.; Oliveira, B. L.; Deery, M. J.; Pukala, T. L.; Perkins, M. V.; Bernardes, G. J. L.; Chalker, J. M. Norbornene probes for the detection of cysteine sulfenic acid in cells. *ACS Chem. Biol.* **2019**, *14*, 594.

(26) Alcock, L. J.; Langini, M.; Stühler, K.; Remke, M.; Perkins, M. V.; Bernardes, G. J. L.; Chalker, J. M. Proteome-wide survey of cysteine oxidation by using a norbornene probe. *ChemBioChem* **2020**, *21*, 1.

(27) Miki, T.; Awa, M.; Nishikawa, Y.; Kiyonaka, S.; Wakabayashi, M.; Ishihama, Y.; Hamachi, I. A conditional proteomics approach to identify proteins involved in zinc homeostasis. *Nat. Methods* **2016**, *13*, 931.

(28) Nishikawa, Y.; Miki, T.; Awa, M.; Kuwata, K.; Tamura, T.; Hamachi, I. Development of a nitric oxide-responsive labeling reagent for proteome analysis of live cells. *ACS Chem. Biol.* **2019**, *14*, 397.

(29) Sikora, A.; Zielonka, J.; Lopez, M.; Joseph, J.; Kalyanaraman, B. Direct oxidation of boronates by peroxynitrite: mechanism and implications in fluorescence imaging of peroxynitrite. *Free Radical Biol. Med.* **2009**, *47*, 1401.

(30) Zhu, Q.; Girish, A.; Chattopadhaya, S.; Yao, S. Q. Developing novel activity-based fluorescent probes that target different classes of proteases. *Chem. Commun.* **2004**, 1512.

(31) Doura, T.; Kamiya, M.; Obata, F.; Yamaguchi, Y.; Hiyama, T. Y.; Matsuda, T.; Fukamizu, A.; Noda, M.; Miura, M.; Urano, Y. Detection of LacZ-positive cells in living tissue with single-cell resolution. *Angew. Chem. Int. Ed.* **2016**, *55*, 9620.

(32) Chiba, M.; Kamiya, M.; Tsuda-Sakurai, K.; Fujisawa, Y.; Kosakamoto, H.; Kojima, R.; Miura, M.; Urano, Y. Activatable photosensitizer for targeted ablation of *lacZ*-positive cells with single-cell resolution. *ACS Cent. Sci.* **2019**, *5*, 1676.

(33) Polaske, N. W.; Kelly, B. D.; Ashworth-Sharpe, J.; Bieniarz, C. Quinone methide signal amplification: covalent reporter labeling of cancer epitopes using alkaline phosphatase substrates. *Bioconjugate Chem.* **2016**, *27*, 660. This work described a QM-based signal amplification method for immunohistochemical assays, which demonstrated the ability of QM for covalent labeling in close proximity within the nucleus.

(34) Zhong, Q.; Ngim, K. K.; Sun, M.; Li, J.; Deese, A.; Chetwyn, N. P. Strategies for the analysis of highly reactive pinacolboronate esters. *J. Chromatogr. A* **2012**, *1229*, 216.

(35) Dickinson, B. C.; Huynh, C.; Chang, C. J. A palette of fluorescent probes with varying emission colors for imaging hydrogen peroxide signaling in living cells. *J. Am. Chem. Soc.* **2010**, *132*, 5906.

(36) Larsen, E. C.; DiGennaro, J. A.; Saito, N.; Mehta, S.; Loegering, D. J.; Mazurkiewicz, J. E.; Lennartz, M. R. Differential requirement for classic and novel PKC isoforms in respiratory burst and phagocytosis in RAW264.7 cells. *J. Immunol.* **2000**, *165*, 2809.

(37) Lundqvist, H.; Folllin, P.; Khalfan, L.; Dahlgren, C. Phorbol myristate acetate-induced NADPH oxidase activity in human neutrophils: only half the story has been told. *J. Leukoc. Biol.* **1996**, *59*, 270.

(38) Bylund, J.; Brown, K. L.; Movitz, C.; Dahlgren, C.; Karlsson, A. Intracellular generation of superoxide by the phagocyte NADPH oxidase: how, where, and what for? *Free Radic. Biol. Med.* **2010**, *49*, 1834.

(39) Dupré-Crochet, S.; Erard, M.; Nüβe, O. ROS production in phagocytes: why, when and where? *J. Leukoc. Biol.* **2013**, *94*, 657.

(40) We also performed the proteomics with a control compound, fluorescein diacetate (FDA), which identified only 15 proteins and none of them showed a significant H/L ratio (Supplementary Fig. 13 and Supplementary Data 3).

(41) Lamb, F. S.; Hook, J. S.; Hilkin, B. M.; Huber, J. N.; Volk, A. P. D.; Moreland, J. G. Endotoxin priming of neutrophils requires endocytosis and NADPH oxidase-dependent endosomal reactive oxygen species. *J. Biol. Chem.* **2012**, *287*, 12395.

(42) Kurz, T.; Terman, A.; Gustafsson, B.; Brunk, U. T. Lysosomes and oxidative stress in aging and apoptosis. *Biochim. Biophys. Acta* **2008**, *1780*, 1291.

(43) Remijsen, Q.; Berghe, T. V.; Wirawan, E.; Asselbergh, B.; Parthoens, E.; Rycke, R. D.; Noppen, S.; Delforge, M.; Willems, J.; Vandenabeele, P. Neutrophil extracellular trap cell death requires both autophagy and superoxide generation. *Cell Res.* **2011**, *21*, 290.

(44) Mitroulis, I.; Kourtzelis, I.; Kambas, K.; Rafail, S.; Chrysanthopoulou, A.; Speletas, M.; Ritis, K. Regulation of the autophagic machinery in human neutrophils. *Eur. J. Immunol.* **2010**, *40*, 1461.

(45) Dröse, S. Differential effects of complex II on mitochondrial ROS production and their relation to cardioprotective pre- and postconditioning. *Biochem. Biophys. Acta* **2013**, *1827*, 578.

(46) Chen, Y.; McMillan-Ward, E.; Kong, J.; Israels, S. J.; Gibson, S. B. Mitochondrial electron-transport-chain inhibitors of complex I and II induce autophagic cell death mediated by reactive oxygen species. *J. Cell Sci.* **2007**, *120*, 4155.

(47) Massaad, C. A.; Klann, E. Reactive oxygen species in the regulation of synaptic plasticity and memory. *Antioxid. Redox Sign.* **2011**, *14*, 2013.

(48) Brennan, A. M.; Suh, S. W.; Won, S. J.; Narasimhan, P.; Kauppinen, T. M.; Lee, H.; Edling, Y.; Chan, P. H.; Swanson, R. A. NADPH oxidase is the primary source of superoxide induced by NMDA receptor activation. *Nat. Neurosci.* **2009**, *12*, 857.

(49) Scherz-Shouval, R.; Shvets, E.; Fass, E.; Shorer, H.; Gil, L.; Elazar, Z. Reactive oxygen species are essential for autophagy and specifically regulate the activity of Atg4. *EMBO J.* **2007**, *26*, 1749.

(50) Lam, G. Y.; Huang, J.; Brumell, J. H. The many roles of NOX2 NADPH oxidase-derived ROS in immunity. *Semin. Immunopathol.* **2010**, *32*, 425.

For Table of Contents Only

Imaging and profiling of proteins under oxidative conditions in cells and tissues by hydrogen-peroxide-responsive labeling